Original Article | Neuroimaging and Head & Neck

eISSN 2005-8330
https://doi.org/10.3348/kjr.2022.0919
Korean J Radiol 2023;24(8):772-783

Korean Journal of Radiology
KJR

Imaging-Based Versus Pathologic Survival Stratifications of Diffuse Glioma According to the 2021 WHO Classification System

So Jeong Lee[1], Ji Eun Park[1], Seo Young Park[2], Young-Hoon Kim[3], Chang Ki Hong[3], Jeong Hoon Kim[3], Ho Sung Kim[1]

[1]Department of Radiology and Research Institute of Radiology, Asan Medical Center, University of Ulsan College of Medicine, Seoul, Republic of Korea
[2]Deparment of Statistics and Data Science, Korea National Open University, Seoul, Republic of Korea
[3]Department of Neurosurgery, Asan Medical Center, University of Ulsan College of Medicine, Seoul, Republic of Korea

Objective: Imaging-based survival stratification of patients with gliomas is important for their management, and the 2021 WHO classification system must be clinically tested. The aim of this study was to compare integrative imaging- and pathology-based methods for survival stratification of patients with diffuse glioma.

Materials and Methods: This study included diffuse glioma cases from The Cancer Genome Atlas (training set: 141 patients) and Asan Medical Center (validation set: 131 patients). Two neuroradiologists analyzed presurgical CT and MRI to assign gliomas to five imaging-based risk subgroups (1 to 5) according to well-known imaging phenotypes (e.g., T2/FLAIR mismatch) and recategorized them into three imaging-based risk groups, according to the 2021 WHO classification: group 1 (corresponding to risk subgroup 1, indicating oligodendroglioma, isocitrate dehydrogenase [IDH]-mutant, and 1p19q-co-deleted), group 2 (risk subgroups 2 and 3, indicating astrocytoma, IDH-mutant), and group 3 (risk subgroups 4 and 5, indicating glioblastoma, IDHwt). The progression-free survival (PFS) and overall survival (OS) were estimated for each imaging risk group, subgroup, and pathological diagnosis. Time-dependent area-under-the receiver operating characteristic analysis (AUC) was used to compare the performance between imaging-based and pathology-based survival model.

Results: Both OS and PFS were stratified according to the five imaging-based risk subgroups ($P < 0.001$) and three imaging-based risk groups ($P < 0.001$). The three imaging-based groups showed high performance in predicting PFS at one-year (AUC, 0.787) and five-years (AUC, 0.823), which was similar to that of the pathology-based prediction of PFS (AUC of 0.785 and 0.837). Combined with clinical predictors, the performance of the imaging-based survival model for 1- and 3-year PFS (AUC 0.813 and 0.921) was similar to that of the pathology-based survival model (AUC 0.839 and 0.889).

Conclusion: Imaging-based survival stratification according to the 2021 WHO classification demonstrated a performance similar to that of pathology-based survival stratification, especially in predicting PFS.

Keywords: Diffuse glioma; Survival; Imaging; Stratification; CNS WHO 2021 classification

INTRODUCTION

The integration of molecular characteristics into the 2021 World Health Organization (WHO) classification facilitates research on imaging correlates for diffuse gliomas, leading to a more precise imaging-based classification. The primary focus of imaging correlates is the prediction of isocitrate dehydrogenase (IDH) mutations and deletion of chromosome arms 1p and 19q (1p19q co-deletion [1p19q-codel]) according to tumor location, necrosis/cysts, calcification, contrast enhancement, and T2/FLAIR mismatch sign [1-5]. The presence of calcifications or cysts is associated with

Received: November 21, 2022 **Revised:** April 5, 2023 **Accepted:** May 20, 2023
Corresponding author: Ji Eun Park, MD, PhD, Department of Radiology and Research Institute of Radiology, Asan Medical Center, University of Ulsan College of Medicine, 88 Olympic-ro 43-gil, Songpa-gu, Seoul 05505, Republic of Korea
• E-mail: jieunp@gmail.com

Korean Journal of Radiology
KJR

1p19q-codel [6]. The T2/FLAIR mismatch sign is associated with IDH-mutant astrocytoma, which also has a negative 1p19q non-co-deletion [4]. A recent study [7] showed that the reproducible imaging parameters for predicting molecular diagnosis included the presence of necrosis, T2/FLAIR mismatch, internal cysts, and predominant contrast enhancement.

Imaging-based survival stratification deserves more attention than just for the prediction of specific molecular diagnoses that allow for survival-stratified management. This is especially the case in patients who undergo a difficult biopsy where tumors are deep or when an insufficient surgical specimen is acquired and an inconclusive molecular diagnosis of not otherwise specified (NOS) is received [8]. However, no single imaging feature is representative of a certain molecular diagnosis, and even a strong imaging parameter such as the T2/FLAIR mismatch sign, which exhibits an almost 100% positive predictive value for IDH-mutant astrocytoma [4], can have low sensitivity and produce false-positive cases [9-12]. Therefore, instead of focusing on the presence of a single specific imaging parameter, imaging-based survival stratification provides an integrative approach using neuroradiologist-defined magnetic resonance imaging (MRI) patterns, including the contrast enhancement pattern, T2/FLAIR mismatch, tumor margin, and tumor location.

The latest 2021 WHO classification no longer uses the term anaplastic for grade 3 tumors, and diffuse astrocytoma, IDH-wild type (IDHwt) (central nervous system [CNS] WHO grade 2 or 3), is a rare entity that is no longer considered a tumor type [13]. For diffuse gliomas in adults, three subtypes remain: oligodendroglioma, IDH-mutant, 1p19q co-deleted (IDHmut/1p19q-codel, CNS WHO 2 and 3); diffuse astrocytoma, IDH-mutant (IDHmut, CNS WHO 2, 3, or 4); and glioblastoma, IDHwt. This revision raises two questions: 1) whether the imaging-based group matches the molecular diagnosis according to the 2021 WHO classification system, and 2) whether the performance of the imaging-based group is similar to the pathologic molecular-based method for survival stratification.

We hypothesized that imaging-based survival stratification in terms of overall survival (OS) and progression-free survival (PFS) would be comparable to pathology-based survival stratification. The aim of this study was to compare integrative imaging- and pathology-based survival models for risk stratification of patients with diffuse gliomas.

MATERIALS AND METHODS

Study Population

This retrospective study was approved by the local ethics committee and institutional review board of the Asan Medical Center (local approval number: 2021-1499), and the requirement for written informed consent was waived. We included 141 patients from The Cancer Genome Atlas (TCGA, https://portal.gdc.cancer.gov) and 131 patients from the Asan Medical Center with WHO grade 2/3/4 diffuse gliomas as the training and validation sets, respectively.

For the training set, we included patients from TCGA who were initially diagnosed with and had untreated WHO grade 2/3/4 diffuse gliomas. The inclusion criterion was the availability of presurgical MRI, which included T1, T2, FLAIR, and contrast-enhanced T1-weighted images. Of the 141 patients, 17 had IDHmut/1p19q-codel, 53 had IDHmut, and 71 had IDHwt, according to the 2021 WHO classification. Survival information was available for all patients.

A validation set was formed from patients with available IDH and 1p19q genetic test results and available pretreatment MRI scans acquired at Asan Medical Center between January 2018 and December 2019. The exclusion criteria were as follows: 1) previous treatment for glioma (n = 20); 2) missing, inconclusive, or ambiguous molecular results (e.g., IDHwt/1p19q-codel; n = 23); 3) prolonged (> 1 year) interval between MRI and surgery (n = 5); and 4) missing images (n = 1). Of the 131 patients, 19 had IDHmut/1p19q-codel, 24 had IDHmut, and 88 had IDHwt, according to the 2021 WHO classification. The included patients are shown in the Strengthening the Reporting of Observational Studies in Epidemiology (STROBE) diagram in Figure 1. The patients in the validation set overlapped with those included in a previous study on identifying imaging parameters for the prediction of pathology-based glioma molecular diagnosis, with a focus on individual imaging parameters without survival information [7].

MRI Acquisition Protocol

The MRI protocols for the training set can be found in a public information repository. For detailed protocols, please refer to www.cancerimagingarchive.net. The MRI protocol for the validation set included the acquisition of T2-weighted, T2-weighted FLAIR, and T1-weighted images obtained before and after the administration of gadolinium-based contrast material. MRI was acquired pre- and post-surgically in all patients (24 examinations at 1.5 T and

https://doi.org/10.3348/kjr.2022.0919

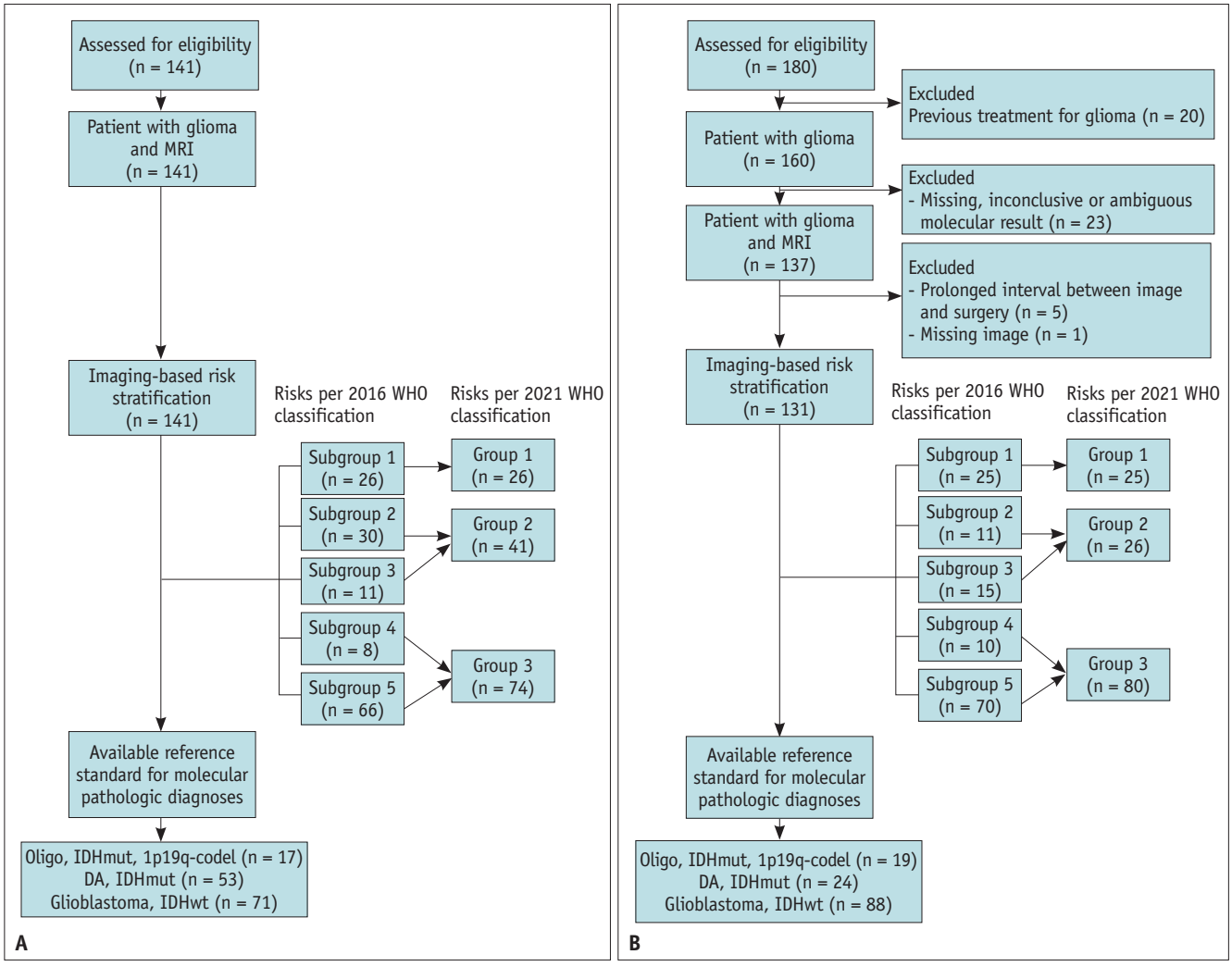

Fig. 1. Study population for the training **(A)** and validation sets **(B)**. Risk groups and subgroups are assigned by readers using imaging-phenotypes. MRI = magnetic resonance imaging, WHO = World Health Organization, Oligo = oligodendroglioma, IDHmut = IDH-mutant, 1p19q-codel = 1p19q co-deleted, DA = diffuse astrocytoma, IDH = isocitrate dehydrogenase, IDHwt = IDH-wild type

107 examinations at 3.0 T). The detailed MRI protocols are provided in Supplementary Table 1.

Imaging Analysis

More than 500 new gliomas are diagnosed per year at Asan Medical Center. Three neuroradiologists with different levels of experience (J.E.P., M.K., and Y.K.N., with seven years, two years, and one year of experience, as readers 1, 2, and 3, respectively) performed image analysis on the training set, and two neuroradiologists (readers 1 and 2) performed image analysis on the validation set. The images were read twice by each reader, that is, six readings per case in the training set (three readers x two times) and four readings in the validation set (two readers x two times). All readers were blinded to clinicopathological information.

The readers independently analyzed and assigned each case to one of the five imaging-based risk subgroups (1–5) according to the WHO 2016 classification by performing an integrative analysis of presurgical computed tomography (CT) and T1-weighted, T2-weighted, FLAIR, and contrast-enhanced T1-weighted images. The five imaging-based risk subgroups are designated as follows: Subgroup 1 represents an imaging-based oligodendroglioma, IDHmut/1p19q-codel, WHO grade 2 or 3, showing a non-enhancing or partially-enhancing localized tumor with an ill-defined margin, cystic change, necrosis, a predominantly frontal lobe location on MRI, and calcifications on CT [5]. Subgroup 2 represents an imaging-based diffuse astrocytoma, IDHmut, WHO grade 2 or 3, showing a non-enhancing or partially-enhancing well-demarcated tumor margin with a T2/FLAIR mismatch sign

https://doi.org/10.3348/kjr.2022.0919

Korean Journal of Radiology
KJR

in the frontal, insular, or temporal lobes [5]. Subgroup 3 represents an imaging-based diffuse astrocytoma, IDHmut, WHO grade 4, exhibiting a predominantly contrast-enhancing tumor with an adjacent well-demarcated T2/FLAIR high-signal intensity tumor margin and necrotic portion [5,14]. Subgroup 4 represents an imaging-based (non-enhancing) glioblastoma, IDHwt, without definite enhancement and exhibits an ill-defined and infiltrative tumor in a parietal or deep cerebral location [5,14]. Subgroup 5 represents an imaging-based (enhancing) glioblastoma, IDHwt, showing a predominantly contrast-enhancing tumor with an ill-defined T2/FLAIR high-signal intensity tumor margin and necrotic portion in a parietal or deep cerebral location [5,14]. Each reader then described the basis for their assignment by recording the MRI features of the contrast enhancement pattern (predominant, partial, or no enhancement), presence of necrosis, presence of the T2/FLAIR mismatch sign, and presence of internal cysts according to previous publications [15-17]. A cyst was defined as a region within the tumor that showed high signal intensity on T2-weighted images with a well-defined margin and no enhancement. Necrosis was defined as a region within the tumor showing high signal intensity on T2-weighted images with irregular margins and no enhancement [7,18]. Based on the 2021 WHO classification, the five imaging-based risk subgroups were further categorized into three risk groups. Subgroup 1 was classified as group 1 (imaging-based oligodendroglioma, IDHmut/1p19q-codel, WHO grade 2 or 3), subgroups 2 and 3 were classified as group 2 (imaging-based diffuse astrocytoma, IDHmut, WHO grade 2/3/4), and subgroups 4 and 5 were classified as group 3 (glioblastoma, IDHwt). Examples of lesions showing typical imaging-based risk subgroups and groups are shown in Figure 2.

In the training set, the subgroup/group designation with the majority of the votes among the three readers was selected. In the validation set, the final assessment was determined by a majority vote among the four interpretations by the two readers.

Survival Data and Modeling

We developed imaging- and pathology-based survival models for adult-type diffuse glioma using Cox proportional hazard regression (see Statistical analysis). Some clinical variables were added to the imaging-based model according to a previous study [19], including age at diagnosis [20], extent of resection, histological type, WHO grade [21], number of cases showing progression, and number of deaths. In contrast to the previous study, our current study was according to the 2021 WHO classification and included three imaging-based risk groups (indicating IDHmut/1p19q-codel, IDHmut, and IDHwt), and previous oligoastrocytoma was assigned to either 'oligodendroglioma, IDHmut/1p19q-codel' or 'diffuse astrocytoma, IDHmut'.

For the training data, OS and PFS data were collected from the TCGA data archive. For the validation data, a neuroradiologist (H.S.K., with 23 years of experience in neuro-oncologic imaging) and a neurosurgeon (J.H.K., with 28 years of experience), who were blinded to the image analysis results, collected the data regarding OS and PFS. PFS was defined as the time from the day of the pre-resection MRI examination to disease progression or death due to any cause, whichever occurred first. Disease progression was assessed using postsurgical T2-weighted FLAIR and contrast-enhanced T1-weighted images according to the Response Assessment in Neuro-Oncology (RANO) criteria [22,23]. OS was defined as the time from the day of the pre-resection MRI examination to the day of death using information registered in the National Health Care Database.

Statistical Analysis

The clinical characteristics were summarized using descriptive statistics. One-way analysis of variance was used for age and chi-square tests were used for all other variables. An agreement was obtained between the imaging-based risk groups and pathological diagnoses in the training set.

PFS and OS were calculated for the five imaging-based risk subgroups and three imaging-based risk groups using the Kaplan-Meier method, and the Kaplan-Meier curves were compared using the log-rank test.

Univariable Cox proportional hazards regression of OS and PFS was performed for the three imaging-based risk groups, pathology-based molecular diagnosis, and clinical variables, as mentioned above in the training set. The clinical variables were obtained from a historical histopathological survival model [19]. Next, a multivariable survival model using imaging-based risk groups combined with clinical variables and a model using pathology-based molecular diagnosis and clinical variables were constructed by selecting reliable features with a P-value < 0.05 in the univariable analysis. The discrimination performance of the survival stratification model was evaluated in the validation set using the area under the time-dependent receiver operating characteristic (ROC) curve. Areas under the time-

 https://doi.org/10.3348/kjr.2022.0919

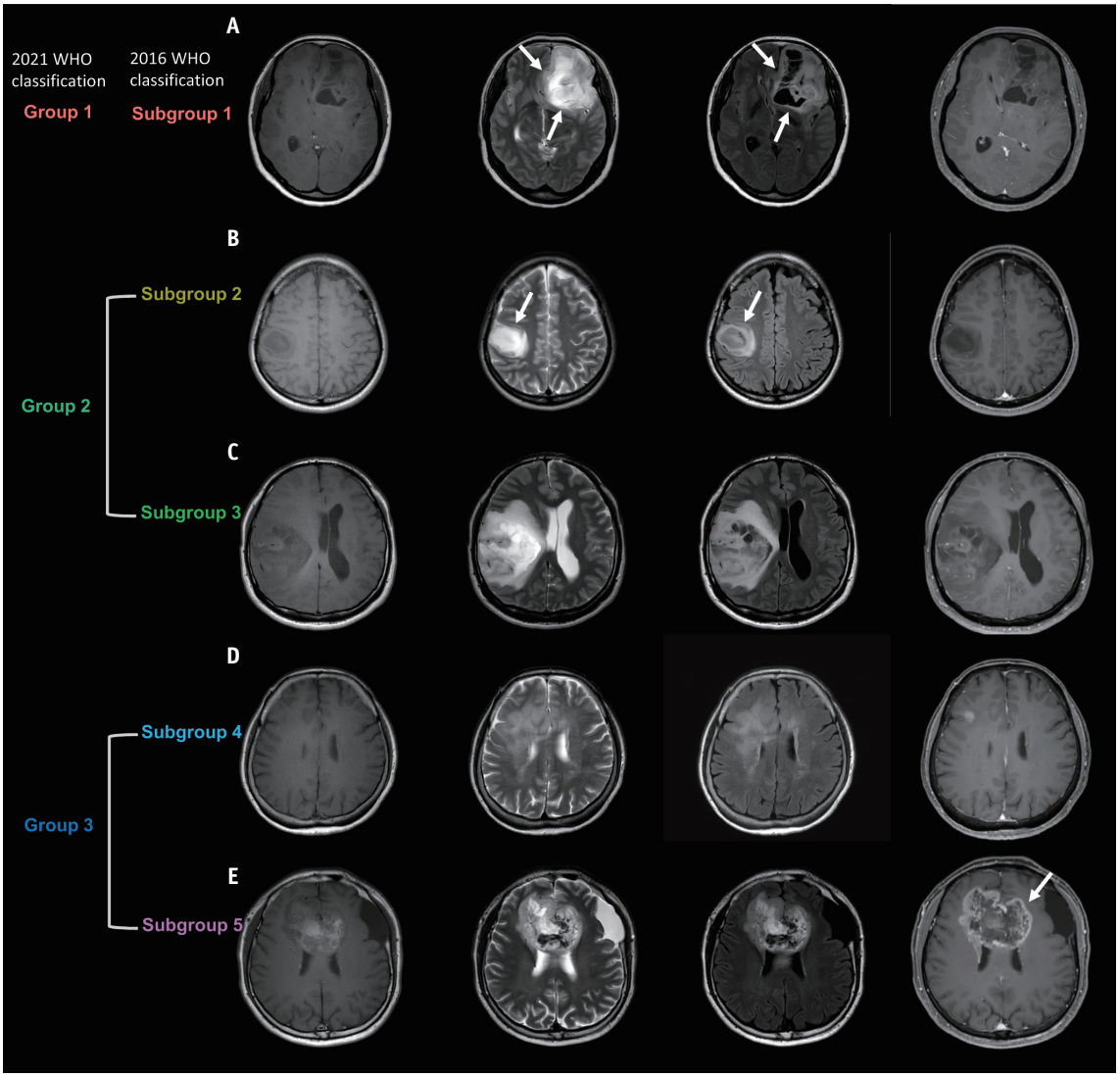

Fig. 2. Examples of imaging-based risk stratification under the 2016 World Health Organization (WHO) classification and the 2021 WHO classification. Demonstration of each major case in the systematic imaging-based risk stratification using T1-weighted, T2-weighted, fluid-attenuated inversion recovery (FLAIR), and contrast-enhanced T1-weighted images. **A:** A 49-year-old female patient in subgroup 1 showing a poorly enhancing mass with internal cysts (arrows) in the left frontal lobe. **B:** A 23-year-old female patient in subgroup 2 showing a T2 high-signal intensity mass with a T2/FLAIR mismatch sign (arrows) in the right parietal lobe. **C:** A 32-year-old male patient in subgroup 3 exhibiting a predominantly contrast-enhancing tumor with an adjacent well-demarcated T2/FLAIR high-signal-intensity tumor margin and a necrotic portion in the right frontoparietal lobe. **D:** A 63-year-old female patient in subgroup 4 exhibiting an ill-defined T2/FLAIR high-signal-intensity mass without enhancement in the left frontal lobe. **E:** A 63-year-old male patient in subgroup 5 showing an irregular, predominantly enhancing mass (arrow) with internal hemorrhage and necrosis in both frontal lobes. 2021 WHO classification: group 1 = imaging phenotypes indicating oligodendroglioma, IDH-mutant, 1p19q co-deleted; group 2 = imaging phenotypes indicating diffuse astrocytoma, IDH-mutant; group 3 = imaging phenotypes indicating glioblastoma, IDH-wild type. IDH = isocitrate dehydrogenase

dependent ROC curves (AUC) for the 1-year, 2-year, 3-year, and 5-year follow-ups were calculated.

Statistical testing was performed by a biostatistician (S.Y.P. with 13 years of experience) using the R software (version 4.0.2., Institute for Statistics and Mathematics, Vienna, Austria, https://www.R-project.org).

RESULTS

Study Population

The patient demographics and clinical characteristics are shown in Table 1. The clinical characteristics of the training and validation sets were similar. The mean age at the time of diagnosis was significantly higher in patients with IDHwt

https://doi.org/10.3348/kjr.2022.0919

Korean Journal of Radiology
KJR

tumors than in those with other molecular diagnoses. There was no significant difference in the sex ratio between the three diagnoses.

Among the imaging predictors, contrast enhancement (90.5%, chi-square, $P < 0.001$) and necrosis (85.1%, $P < 0.001$) were the most common features in the IDHwt tumors in both the training and validation sets. Contrast enhancement was the most common feature in IDHwt tumors in both the training (57.7%, $P < 0.001$) and validation (93.2%, $P < 0.001$) sets. The presence of a T2/FLAIR mismatch in the training (32.1%, $P < 0.001$) and validation (33.3%, $P < 0.001$) sets was observed primarily in IDHmut.

Concordance of Imaging-Based Molecular Subtypes with Actual Pathology

A concordance table comparing the pathology- and imaging-based risk subgroup (group 1 to 5) for each individual reader and number of reading is provided in Supplementary Table 2. The concordance index (accuracy) for classification was 56.3% (476/846) for the training set and 79.8% (418/524) for the validation set.

Figure 3 shows the imaging-based survival stratification in the validation set according to the majority vote of the two readers, depicted according to the three risk groups (2021 WHO classification) and five imaging-based risk subgroups. PFS and OS were significantly different among the groups and subgroups (log-rank test, largest $P < 0.001$).

Imaging-Based and Pathology-Based Survival Prediction

The univariable and multivariable Cox proportional hazards regression results for PFS and OS are shown in Table 2. Significant predictors of PFS in the multivariable analysis were subtotal resection, partial resection or biopsy (hazard ratio [HR] = 1.59; 95% confidence interval [CI]: 1.04–2.42, $P = 0.032$), higher WHO grade (grade 3 or 4, HR = 2.42; 95% CI: 1.9–4.93, $P = 0.015$), and imaging-based risk group 3 (indicating IDHwt) (HR = 6.93; 95% CI: 2.53–18.94, $P < 0.001$). Significant predictors of OS in the multivariable analysis were subtotal resection, partial resection or biopsy (HR = 1.87; 95% CI: 1.15–3.02, $P = 0.011$), higher WHO grade (grade 3 or 4, HR = 3.97; 95% CI: 1.44–10.99, $P = 0.008$), and imaging-based risk group 3 (indicating IDHwt)

Table 1. Patient and lesion characteristics according to pathologic diagnosis

	Training set			Validation set		
	IDHmut/ 1p19q-codel (n = 17)	IDHmut (n = 53)	IDHwt (n = 71)	IDHmut/ 1p19q-codel (n = 19)	IDHmut (n = 24)	IDHwt (n = 88)
Age at diagnosis (yr)	50.1 ± 11.9	41 ± 13.9	56.4 ± 14.4	45.8 ± 10.9	41.6 ± 12.7	58.4 ± 11.6
Sex, Male	9 (52.9)	30 (56.6)	44 (62.0)	15 (78.9)	11 (45.8)	49 (55.7)
Imaging feature						
Contrast enhancement	10 (58.8)	31 (58.5)	41 (57.7)	2 (10.5)	8 (33.3)	82 (93.2)
Necrosis	9 (52.9)	11 (20.8)	37 (52.1)	0 (0)	5 (20.8)	77 (87.5)
Cyst	12 (70.6)	17 (32.1)	3 (4.2)	12 (63.2)	8 (33.3)	10 (11.4)
T2/FLAIR mismatch	1 (5.9)	17 (32.1)	2 (2.8)	0 (0)	8 (33.3)	1 (1.1)
Location						
Multilobar	1 (5.9)	5 (9.4)	24 (33.8)	0 (0)	0 (0)	6 (6.8)
Isolated	15 (88.2)	38 (71.7)	12 (16.9)	19 (100)	23 (95.8)	77 (87.5)
Other*	1 (5.9)	10 (18.9)	35 (49.3)	0 (0)	1 (4.2)	5 (5.7)
WHO grade						
2	7 (41.2)	25 (47.2)	0 (0)	19 (100)	16 (66.7)	0 (0)
3	10 (58.8)	23 (43.4)	0 (0)	0 (0)	0 (0)	0 (0)
4	0 (0)	5 (9.4)	71 (100)	0 (0)	8 (33.3)	88 (100)
Number of cases showing progression	5 (29.4)	15 (28.3)	55 (77.5)	3 (15.8)	12 (50)	68 (77.3)
Number of deaths	4 (23.5)	6 (11.3)	53 (74.6)	0 (0)	7 (29.2)	65 (73.9)

Values are presented as mean ± standard deviation or n (%) unless otherwise indicated.
*Other location includes thalamus, basal ganglia and cerebellum.
IDH = isocitrate dehydrogenase, mut = mutant, wt = wild type, 1p19q = chromosome arms 1p and 19q, codel = co-deletion, FLAIR = fluid-attenuated inversion recovery, WHO = World Health Organization

https://doi.org/10.3348/kjr.2022.0919

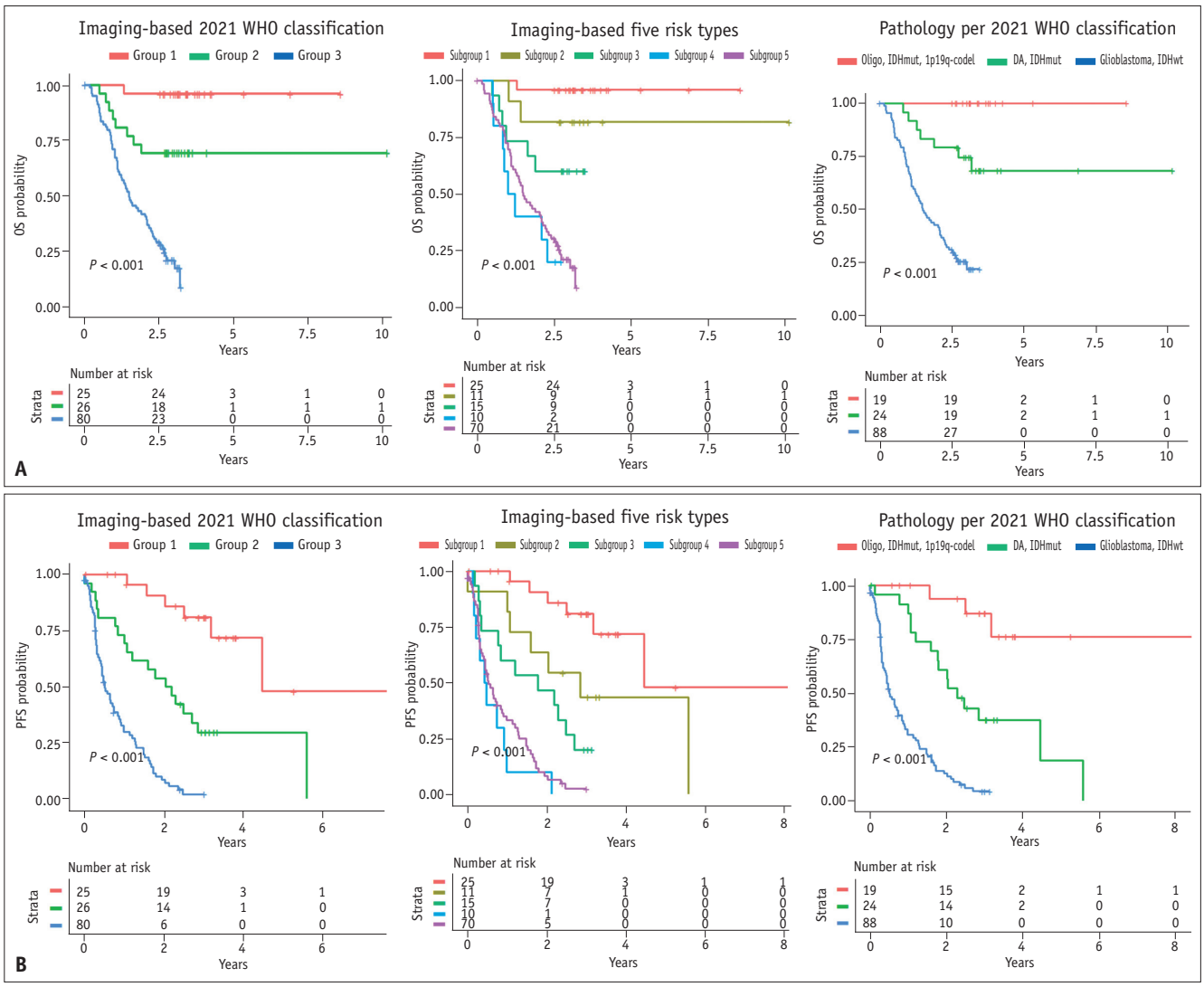

Fig. 3. Stratification of **(A)** overall survival (OS) and **(B)** progression-free survival (PFS) in the validation set according to the three imaging-based risk groups based on 2021 World Health Organization (WHO) classification (left), the five imaging-based risk subgroups (middle), and pathology according to the 2021 WHO classification (right). Oligo = oligodendroglioma, IDHmut = isocitrate dehydrogenase (IDH) mutant, 1p19q-codel = chromosome arms 1p and 19q co-deleted, DA = diffuse astrocytoma, IDHwt = IDH-wild type

(HR = 15.21; 95% CI: 1.80–128.37, P = 0.012). Based on the results of the multivariable Cox regression analysis, we constructed a survival model using imaging-based risk groups and clinical predictors.

The results of the time-dependent ROC curve analysis of the imaging-based risk groups and pathological diagnoses are shown in Table 3. The imaging-based risk groups showed high performance in predicting PFS at one year (AUC, 0.787; 95% CI: 0.716–0.858) and five years (AUC, 0.823; 95% CI: 0.700–0.946). This was similar to the pathology-based survival prediction, which showed a 1-year AUC of 0.785 (95% CI: 0.719–0.851) and a 5-year AUC of 0.837 (95% CI: 0.761–0.912) for PFS. The imaging-based risk groups showed low performance in the prediction of OS at one year (AUC 0.667, 95% CI: 0.589–0.744), but showed high performance at five years (0.952, 95% CI: 0.903–1.000). In the pathology-based survival model, OS could not be calculated because no death events occurred in the oligodendroglioma, IDH-mutant, or 1p19q-codel subtypes. The results of the time-dependent ROC curve analysis of the imaging-based survival model are shown in Figure 4.

After combining the clinical parameters, the combined imaging-based survival model for PFS demonstrated AUCs of 0.813 (95% CI: 0.735–0.890) and 0.921 (95% CI: 0.863–0.979) at one and three years, respectively. The corresponding combined pathology-based survival model

https://doi.org/10.3348/kjr.2022.0919

Korean Journal of Radiology
KJR

Table 2. Cox regression analysis of overall survival and PFS for the imaging-based risk groups and clinical parameters in the training set

Parameter	Overall survival				Progression-free survival			
	Univariable analysis		Multivariable analysis		Univariable analysis		Multivariable analysis	
	HR (95% CI)	*P*	HR (95% CI)	*P*	HR (95% CI)	*P*	HR (95% CI)	*P*
Age at diagnosis (per 5 years)	1.17 (1.06, 1.28)	0.001	1.03 (0.94, 1.13)	0.574	1.14 (1.05, 1.23)	< 0.001	1.02 (0.94, 1.1)	0.660
Extent of resection								
Gross total	ref		ref		ref		ref	
< Gross total	0.91 (0.57, 1.44)	0.676	1.87 (1.15, 3.02)	0.011	0.88 (0.59, 1.31)	0.525	1.59 (1.04, 2.42)	0.032
WHO grade								
2	ref		ref		ref		ref	
3 or 4	9.98 (4.0, 24.95)	< 0.001	3.97 (1.44, 10.99)	0.008	5.55 (3.1, 9.95)	< 0.001	2.42 (1.9, 4.93)	0.015
Imaging-based risk groups (per WHO 2021)								
Group 1	ref		ref		ref		ref	
Group 2	11.27 (1.46, 87.31)	0.02	6.10 (0.72, 51.37)	0.096	3.05 (1.29, 7.22)	0.011	2.39 (0.94, 6.07)	0.067
Group 3	37.92 (5.22, 275.50)	< 0.001	15.21 (1.80, 128.37)	0.012	11.75 (5.16, 26.75)	< 0.001	6.93 (2.53, 18.94)	< 0.001

PFS = progression-free survival, HR = hazard ratio, CI = confidence interval, WHO = World Health Organization, ref = reference

for PFS showed 1-year and 3-year AUCs of 0.839 (95% CI: 0.767–0.911) and 0.889 (95% CI: 0.784–0.993), respectively. Compared with the pathology-based survival models, the imaging-based models showed a tendency of lower performance according to the 1-year AUC, but better performance according to the 3-year AUC. For OS, the combined imaging-based model showed high performance, with AUCs of 0.734 (95% CI: 0.642–0.826) and 0.915 (95% CI: 0.857–0.973) at one and three years, respectively.

DISCUSSION

In this study, diffuse gliomas were assigned to imaging-based risk groups according to the 2021 WHO classification system. This categorization used an integrative analysis that considered the contrast enhancement pattern, T2/FLAIR mismatch, tumor margin, and tumor location. The performance of the survival model demonstrated that imaging-based risk groups could stratify patients according to survival and predict both PFS and OS. For prognostication over one and three years, the imaging-based survival model showed a similar performance to the pathology-based model, especially for PFS. Our study demonstrated that imaging-based risk assessment may be helpful for patient prognostication and consultation when a molecular diagnosis is not available.

With the growing importance of molecular analysis of diffuse gliomas for managing treatment, determining treatment options, and predicting prognosis [24,25], accomplishing a complete molecular diagnosis has become challenging. For patients with inoperable conditions or those with deeply located tumors, obtaining sufficient biospecimens for next-generation sequencing may not be possible. Moreover, a proportion of patients are diagnosed with NOS either because testing is not performed, or the assay results are inconclusive because of an insufficient specimen [8]. For such patients, an imaging-based risk assessment relevant to the molecular diagnosis of diffuse gliomas may be helpful for patient consultation and providing prognostic information. Using our image-based survival stratification, patients with features indicative of aggressiveness, such as necrosis or predominant contrast enhancement, are likely to be assigned to the imaging-based glioblastoma IDHwt group, which provides guidance for early treatment planning and patient consultation.

A previous study reported excellent performance in predicting pathology based on imaging features and

https://doi.org/10.3348/kjr.2022.0919

Table 3. Comparison of discrimination performance between imaging-based survival model and pathology-based survival model in the validation set

	Imaging-based survival model			
	1-year AUC	2-year AUC	3-year AUC	5-year AUC
PFS				
Single parameter				
Imaging-based risk groups	0.787 (0.716–0.858)	0.850 (0.779–0.922)	0.884 (0.811–0.956)	0.823 (0.700–0.946)
Age	0.623	0.690	0.761	0.655
Extent of resection	0.513	0.587	0.565	0.585
WHO grade	0.712	0.777	0.843	0.823
Combined model	0.813 (0.735–0.890)	0.882 (0.811–0.953)	0.921 (0.863–0.979)	0.865 (0.754–0.977)
OS				
Single parameter				
Imaging-based risk groups	0.667 (0.589–0.744)	0.712 (0.638–0.786)	0.870 (0.799–0.940)	0.952 (0.903–1.000)
Age	0.618	0.662	0.735	0.797
Extent of resection	0.455	0.447	0.537	0.660
WHO grade	0.666	0.697	0.807	0.966
Combined model	0.734 (0.642–0.826)	0.800 (0.726–0.875)	0.915 (0.857–0.973)	0.990 (0.972–1.000)
	Pathology-based survival model			
	1-year AUC	2-year AUC	3-year AUC	5-year AUC
PFS				
Single parameter				
Pathologic molecular diagnoses	0.785 (0.719–0.851)	0.828 (0.750–0.906)	0.894 (0.812–0.976)	0.837 (0.761–0.912)
Age	0.623	0.690	0.761	0.655
Extent of resection	0.513	0.587	0.565	0.585
WHO grade	0.712	0.777	0.843	0.823
Combined model	0.839 (0.767–0.911)	0.829 (0.740–0.918)	0.889 (0.784–0.993)	0.975 (0.743–0.999)
OS	NA	NA	NA	NA

Combined model includes all the single parameters as predictors. Numbers in parentheses are 95% confidence intervals. The AUC of OS for pathologic-based survival model was not calculable because of the lack of deaths in type 1.
AUC = area under the receiver operating characteristics curve, PFS = progression-free survival, WHO = World Health Organization, OS = overall survival, NA = not applicable

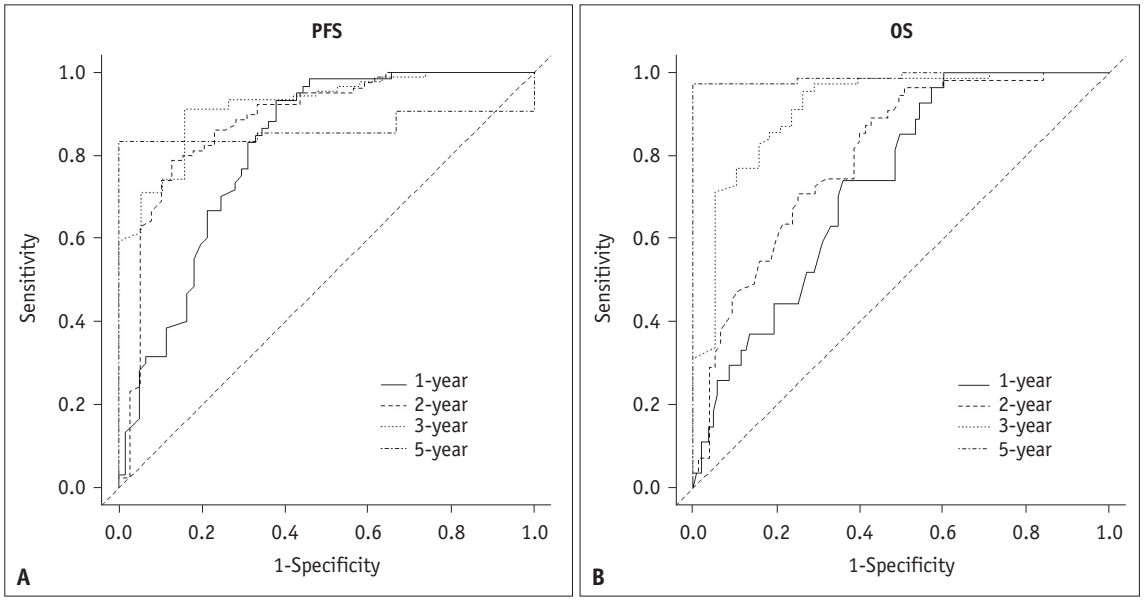

Fig. 4. Performance of the imaging-based survival model. Time-dependent receiver operating characteristic curves of the imaging-based survival model for progression-free survival (PFS; **A**) and overall survival (OS; **B**) in the validation set.

https://doi.org/10.3348/kjr.2022.0919

Korean Journal of Radiology
KJR

demonstrated excellent diagnostic performance for predicting IDHwt type glioblastoma [7]. Additionally, for diffuse glioma NOS, a survival model based on imaging features stratified according to risk showed excellent predictive performance [26]. Several studies have used imaging features for survival stratification. In low-grade gliomas, the presence of enhancement and irregular margins are associated with a shorter PFS [17]. In glioblastomas, survival is shorter if the tumor is large and enhanced [27]. In a study by Nicolasjilwan et al. [28], strong enhancement and a high T1/FLAIR ratio were associated with shorter survival times. A high T1/FLAIR ratio indicated an infiltrative tumor. If the glioblastoma is located in the frontal lobe or on the right side, patients tend to have a longer survival time. In contrast, when gliomas are found in a periventricular location, the prognosis tends to be worse [29,30]. According to Pope et al. [31], a patient has a higher life expectancy if there is no enhancement or edema around a high-grade glioma without satellites or multifocal lesions.

In this study, we focused on developing an integrative imaging-based survival stratification of tumors rather than determining whether individual imaging parameters are diagnostic for certain molecular types. Such survival stratification can fulfill clinical needs when a reference standard is unavailable [32] and time-to-event data are important. Applying a majority vote to imaging risks mimics clinical practice in the reading room and practical methods used in the routine reading of CT and MRI by physicians. Decisions based on integrative imaging-based risk stratification include analysis of the imaging features of necrosis, T2/FLAIR mismatch, presence of internal cysts, and predominant contrast enhancement, which show high reproducibility [7] across readers with different levels of experience.

Predicting early progression using PFS also predicts survival [33,34] and is especially helpful in glioblastoma [33]. Importantly, imaging-based survival stratification showed high performance for 1-year PFS and long-term survival over three years. The high performance obtained using the three imaging-based risk groups according to the 2021 WHO classification supports the findings of a previous study that used a historical pathologic-survival model [19] and showed that the three molecular diagnoses based on IDH mutation and 1p19q-codel status are valid. The high performance of imaging features in determining PFS indicates that imaging can be used not only to evaluate morphological changes noninvasively but also to provide a comprehensive assessment of gliomas with spatial heterogeneity [3,5]. Furthermore, imaging features have additional advantages in the current era where biospecimen-based diagnosis is the standard of care.

Our study has several limitations. First, we used data collected retrospectively. Second, although pathological examinations were available for all patients, cases assigned to the 2021 WHO classification-based molecular diagnoses were not assigned according to the examination of the cyclin dependent kinase inhibitor 2A/B (CDKN2A/B) gene, epidermal growth factor receptor (EGFR), chromosome 7 gain/10 loss, or human telomerase reverse transcriptase [35] gene promoter mutation. Third, calcification was not assessed because the imaging phenotypes in this study were based on a structured reporting system using MRI. Further studies incorporating CT findings may strengthen our results. Finally, selecting a patient cohort that included tumors in a deep location or inoperable tumors would have enhanced the clinical value of this study. Nonetheless, this study was the first to demonstrate imaging-based survival stratification according to the 2021 WHO classification system.

In conclusion, imaging-based survival stratification according to the 2021 WHO classification demonstrated a performance similar to that of pathology-based survival stratification, especially for predicting PFS, and may help guide treatment planning for patients, especially when a pathologic molecular diagnosis is difficult to obtain.

Supplement

The Supplement is available with this article at https://doi.org/10.3348/kjr.2022.0919.

Availability of Data and Material

The datasets generated or analyzed during the study are available from the corresponding author on reasonable request.

Conflicts of Interest

Dr. Ji Eun Park and Dr. Ho Sung Kim, the contributing editors of the *Korean Journal of Radiology*, and Prof. Seo Young Park, the Statistical Consultant of *Korean Journal of Radiology*, were not involved in the editorial evaluation or decision to publish this article. All remaining authors have declared no conflicts of interest.

Author Contributions

Conceptualization: Ji Eun Park, Ho Sung Kim. Data curation: So Jeong Lee, Young-Hoon Kim, Chang Ki Hong, Jeong Hoon Kim. Formal analysis: Ji Eun Park, Seo Young Park, Young-Hoon Kim, Chang Ki Hong, Ho Sung Kim. Investigation: So Jeong Lee, Ji Eun Park, Seo Young Park, Ho Sung Kim. Methodology: Ji Eun Park, Seo Young Park. Project administration: Jeong Hoon Kim. Supervision: Ho Sung Kim. Visualization: So Jeong Lee. Writing—original draft: So Jeong Lee. Writing—review & editing: Ji Eun Park, Ho Sung Kim.

ORCID IDs

So Jeong Lee
https://orcid.org/0000-0002-5673-7365
Ji Eun Park
https://orcid.org/0000-0002-4419-4682
Seo Young Park
https://orcid.org/0000-0002-2702-1536
Young-Hoon Kim
https://orcid.org/0000-0002-8852-6503
Chang Ki Hong
https://orcid.org/0000-0002-2761-0373
Jeong Hoon Kim
https://orcid.org/0000-0001-7131-4523
Ho Sung Kim
https://orcid.org/0000-0002-9477-7421

Funding Statement

This research was supported by a grant from the Ministry of Health &Welfare, Republic of Korea (grant number: HI21C1161 and HI22C0471).

Acknowledgments

We thank to Yeo Kyung Nam, MD (Shinchon Yonsei Hospital) and Minjae Kim, MD, PhD (Asan Medical Center) for participating as a reader of this study.

REFERENCES

1. Hammoud MA, Sawaya R, Shi W, Thall PF, Leeds NE. Prognostic significance of preoperative MRI scans in glioblastoma multiforme. *J Neurooncol* 1996;27:65-73
2. Lacroix M, Abi-Said D, Fourney DR, Gokaslan ZL, Shi W, DeMonte F, et al. A multivariate analysis of 416 patients with glioblastoma multiforme: prognosis, extent of resection, and survival. *J Neurosurg* 2001;95:190-198
3. Diehn M, Nardini C, Wang DS, McGovern S, Jayaraman M, Liang Y, et al. Identification of noninvasive imaging surrogates for brain tumor gene-expression modules. *Proc Natl Acad Sci U S A* 2008;105:5213-5218
4. Patel SH, Poisson LM, Brat DJ, Zhou Y, Cooper L, Snuderl M, et al. T2-FLAIR mismatch, an imaging biomarker for IDH and 1p/19q status in lower-grade gliomas: a TCGA/TCIA project. *Clin Cancer Res* 2017;23:6078-6085
5. Smits M, van den Bent MJ. Imaging correlates of adult glioma genotypes. *Radiology* 2017;284:316-331
6. Carrillo JA, Lai A, Nghiemphu PL, Kim HJ, Phillips HS, Kharbanda S, et al. Relationship between tumor enhancement, edema, IDH1 mutational status, MGMT promoter methylation, and survival in glioblastoma. *AJNR Am J Neuroradiol* 2012;33:1349-1355
7. Nam YK, Park JE, Park SY, Lee M, Kim M, Nam SJ, et al. Reproducible imaging-based prediction of molecular subtype and risk stratification of gliomas across different experience levels using a structured reporting system. *Eur Radiol* 2021;31:7374-7385
8. Louis DN, Wesseling P, Paulus W, Giannini C, Batchelor TT, Cairncross JG, et al. cIMPACT-NOW update 1: Not Otherwise Specified (NOS) and Not Elsewhere Classified (NEC). *Acta Neuropathol* 2018;135:481-484
9. Juratli TA, Tummala SS, Riedl A, Daubner D, Hennig S, Penson T, et al. Radiographic assessment of contrast enhancement and T2/FLAIR mismatch sign in lower grade gliomas: correlation with molecular groups. *J Neurooncol* 2019;141:327-335
10. Lee MK, Park JE, Jo Y, Park SY, Kim SJ, Kim HS. Advanced imaging parameters improve the prediction of diffuse lower-grade gliomas subtype, IDH mutant with no 1p19q codeletion: added value to the T2/FLAIR mismatch sign. *Eur Radiol* 2020;30:844-854
11. Johnson DR, Kaufmann TJ, Patel SH, Chi AS, Snuderl M, Jain R. There is an exception to every rule-T2-FLAIR mismatch sign in gliomas. *Neuroradiology* 2019;61:225-227
12. Onishi S, Yamasaki F, Takano M, Yonezawa U, Taguchi A, Sugiyama K, et al. NIMG-01. T2wi-Flair mismatch sign in lower grade glioma and dysembryoplastic neuroepithelial tumor. *Neuro Oncol* 2019;21(Suppl 6):vi161
13. Gritsch S, Batchelor TT, Gonzalez Castro LN. Diagnostic, therapeutic, and prognostic implications of the 2021 World Health Organization classification of tumors of the central nervous system. *Cancer* 2022;128:47-58
14. Arevalo O, Valenzuela R, Esquenazi Y, Rao M, Tran B, Zhu J, et al. The 2016 World Health Organization classification of tumors of the central nervous system: a practical approach for gliomas, part 2. Isocitrate dehydrogenase status-imaging correlation. *Neurographics* 2017;7:344-349
15. Kanazawa T, Fujiwara H, Takahashi H, Nishiyama Y, Hirose Y, Tanaka S, et al. Imaging scoring systems for preoperative molecular diagnoses of lower-grade gliomas. *Neurosurg Rev* 2019;42:433-441
16. Maynard J, Okuchi S, Wastling S, Busaidi AA, Almossawi O, Mbatha W, et al. World Health Organization Grade II/III glioma molecular status: prediction by MRI morphologic features and

apparent diffusion coefficient. *Radiology* 2020;296:111-121
17. Zhou H, Vallières M, Bai HX, Su C, Tang H, Oldridge D, et al. MRI features predict survival and molecular markers in diffuse lower-grade gliomas. *Neuro Oncol* 2017;19:862-870
18. Kim YJ, Chang KH, Song IC, Kim HD, Seong SO, Kim YH, et al. Brain abscess and necrotic or cystic brain tumor: discrimination with signal intensity on diffusion-weighted MR imaging. *AJR Am J Roentgenol* 1998;171:1487-1490
19. Cancer Genome Atlas Research Network; Brat DJ, Verhaak RG, Aldape KD, Yung WK, Salama SR, et al. Comprehensive, integrative genomic analysis of diffuse lower-grade gliomas. *N Engl J Med* 2015;372:2481-2498
20. Buckner JC, Shaw EG, Pugh SL, Chakravarti A, Gilbert MR, Barger GR, et al. Radiation plus procarbazine, CCNU, and vincristine in low-grade glioma. *N Engl J Med* 2016;374:1344-1355
21. Bell EH, Pugh SL, McElroy JP, Gilbert MR, Mehta M, Klimowicz AC, et al. Molecular-based recursive partitioning analysis model for glioblastoma in the temozolomide era: a correlative analysis based on NRG oncology RTOG 0525. *JAMA Oncology* 2017;3:784-792
22. Leao DJ, Craig PG, Godoy LF, Leite CC, Policeni B. Response assessment in neuro-oncology criteria for gliomas: practical approach using conventional and advanced techniques. *Am J Neuroradiol* 2020;41:10-20
23. Wen PY, Macdonald DR, Reardon DA, Cloughesy TF, Sorensen AG, Galanis E, et al. Updated response assessment criteria for high-grade gliomas: response assessment in neuro-oncology working group. *J Clin Oncol* 2010;28:1963-1972
24. Wesseling P, Capper D. WHO 2016 classification of gliomas. *Neuropathol Appl Neurobiol* 2018;44:139-150
25. Louis DN, Perry A, Reifenberger G, von Deimling A, Figarella-Branger D, Cavenee WK, et al. The 2016 World Health Organization classification of tumors of the central nervous system: a summary. *Acta Neuropathol* 2016;131:803-820
26. Jang EB, Kim HS, Park JE, Park SY, Nam YK, Nam SJ, et al. Diffuse glioma, not otherwise specified: imaging-based risk stratification achieves histomolecular-level prognostication. *Eur Radiol* 2022;32:7780-7788
27. Gutman DA, Cooper LA, Hwang SN, Holder CA, Gao J, Aurora TD, et al. MR imaging predictors of molecular profile and survival: multi-institutional study of the TCGA glioblastoma data set. *Radiology* 2013;267:560-569
28. Nicolasjilwan M, Hu Y, Yan C, Meerzaman D, Holder CA, Gutman D, et al. Addition of MR imaging features and genetic biomarkers strengthens glioblastoma survival prediction in TCGA patients. *J Neuroradiol* 2015;42:212-221
29. Chaichana K, Parker S, Olivi A, Quiñones-Hinojosa A. A proposed classification system that projects outcomes based on preoperative variables for adult patients with glioblastoma multiforme. *J Neurosurg* 2010;112:997-1004
30. Zhao K, Liu R, Li Z, Liu M, Zhao Y, Xue Z, et al. The imaging features and prognosis of gliomas involving the subventricular zone: an MRI study. *Clin Neurol Neurosurg* 2022;222:107465
31. Pope WB, Sayre J, Perlina A, Villablanca JP, Mischel PS, Cloughesy TF. MR imaging correlates of survival in patients with high-grade gliomas. *AJNR Am J Neuroradiol* 2005;26:2466-2474
32. Katki HA. Quantifying risk stratification provided by diagnostic tests and risk predictions: comparison to AUC and decision curve analysis. *Stat Med* 2019;38:2943-2955
33. Han KL, Ren M, Wick W, Abrey L, Das A, Jin J, et al. Progression-free survival as a surrogate endpoint for overall survival in glioblastoma: a literature-based meta-analysis from 91 trials. *Neuro Oncol* 2014;16:696-706
34. Lamborn KR, Yung WK, Chang SM, Wen PY, Cloughesy TF, DeAngelis LM, et al. Progression-free survival: an important end point in evaluating therapy for recurrent high-grade gliomas. *Neuro Oncol* 2008;10:162-170
35. Dosovitskiy A, Beyer L, Kolesnikov A, Weissenborn D, Zhai X, Unterthiner T, et al. An image is worth 16x16 words: transformers for image recognition at scale. *arXiv*:2010.11929 [Preprint]. [posted October 22, 2020; revised June 3, 2021; cited October 6, 2021]. https://arxiv.org/abs/2010.11929

 https://doi.org/10.3348/kjr.2022.0919